Proceeding of the 2004 American Control Conference
Boston, Massachusetts June 30 - July 2, 2004

Optimal and Robust Design of Unstable Valve

Qinghui Yuan and Perry Li

Abstract— **Our research is concerned with the design of a cost effective single stage direct acting electrohydraulic valves for high flow rate and high bandwidth applications by utilizing the instability caused by flow induced forces. In our past research, we have demonstrated simple change in valve geometry can be used to manipulate both transient flow force as well as steady flow force for this purpose. In this paper, with the goal of minimizing the steady flow forces range, we present two optimal design methods over the space of these design parameters: (1) the nominal optimal design method, in which no uncertainty is taken into account; (2) the robust optimal design method, in which the design must be robust enough to model uncertainty and perturbations. By representing the original problem as a LFT interconnection, the robust design problem can be formulated into synthesizing an optimal controller for an appropriate static plant with an structured uncertainty. An algorithm is then presented to transform the LFT into an appropriate robust control problem and synthesize the controller. The case study shows that unlike the nominal optimal solutions where viscosity effect is exclusively utilized, the robust optimal solutions tend to take advantage of both viscosity effect and non-orifice flux effect, and in return provide the better performance over nominal optimal solutions.**

I. INTRODUCTION

In single stage direct acting electrohydraulic valves, the main spools are stroked directly by solenoid actuators. They have the the advantages over multi-stage electrohydraulic valves in being low cost, easy to maintain and insensitive to contamination. However, in the high flow rate and high frequency applications, the force and power requirement for the solenoid actuators become prohibitive due to the significant flow induced forces. The approach we adopt is to propose new valve geometries that utilize the fluid flow force induced instability to enhance the spool agility without increasing the requirements on the solenoid actuators. By subsequently stabilizing the spool via feedback control, both the dynamic response and flow rating of single stage valves can be practically improved.

In our past research, we have demonstrated that simple changes in valve geometry can be used to manipulate both the transient flow force as well as the steady flow force to induce spool instability. The unstable phenomena are largely controlled by the following design parameters: 1) the damping length L, 2) a geometry constant α determined by the inner and outer radii of the chamber, and 3) the non-metering orifice constant C determined by the angles of the non-orifice ports to the spool axis. Both the sign and magnitude of the transient flow force induced damping coefficient are directly associated with $\pm L$ [1], [2], [3], the viscosity induced stable/unstable steady flow force is manipulated by αL [4], and the non-orifice flux component of the stable/unstable steady flow force is controlled by C [5].

The problem that this paper addresses is how to choose these design parameters L, C and α such that both the steady flow force (that the solenoid actuator must act against) and the entire valve dimension are minimized. In addition, the design must be robust to model uncertainties, flow ranges, and variation in operating conditions such as operating pressures, temperature, fluid viscosity. It is shown that the original non-convex nominal optimization problem, can be decomposed into several simple convex optimization problems.

The robust optimal design problem is posed as a min-max optimization similar to that in a robust control theory. By showing that the relationship between design parameters, perturbations, and the objective function can be represented as a linear fractional transformation (LFT) interconnection, the valve design problem of finding the optimal set of geometric parameters becomes equivalent to that one of designing an optimal robust performance controller for an appropriate static plant with an structured uncertainty. This reformulation then enables us to apply an extension of the result in [6] for static plants to our problem. The optimal solution based on this approach is then compared to nominal optimal solution. The study shows that in the presence of perturbations, the unstable valve should utilize both the viscosity effect and non-orifice effect to minimize the steady force range. This is a different answer to the perturbation free case, in which the viscosity effect is exclusively utilized to zero out the steady flow forces over the full range of the orifice opening.

The rest of this paper is organized as follows. In section II, the nominal optimal design over the space of the design parameters is addressed, without considering perturbations. Section III presents the robust optimal design methodology. In section IV, a case study of comparing the nominal optimal design with the robust optimal design is provided. Concluding remarks are presented in section V.

II. NOMINAL OPTIMAL DESIGN

Fig. 1 is a critically centered four way flow control valve under consideration. The resultant steady flow force that a valve spool experiences is given by [5]:

$$F_{steady} = sgn(A_o)CQ^2 - 2\frac{\rho\cos\theta}{c_c A_o}Q^2 - \alpha L\mu Q \qquad (1)$$

This research is supported by the National Science Foundation ENG/CMS-0088964.

Q. Yuan and P. Y. Li are with the Department of Mechanical Engineering, University of Minnesota, Minneapolis, MN 55455. E-mails: {qhyuan, pli}@me.umn.edu. Please send all correspondence to Professor Perry Y. Li.

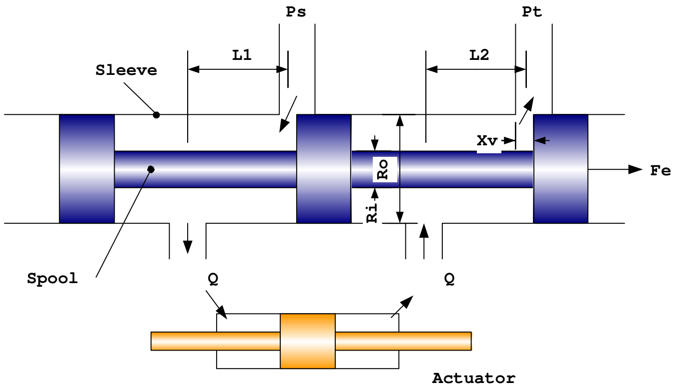

Fig. 1. Typical configuration of a four way direction flow control valve. Two "Q" ports are connected to the load (hydraulic actuator), and P_s is connected to the supply pressure, and P_t is connected to the return. In a single stage valve the spool is stroked directly by solenoid actuators. Damping length L is defined to be $L := L_2 - L_1$. A geometry constant α that is used to determine the viscosity effect of the steady flow forces can be calculated by $\frac{4(2R_o^2 \ln(R_o/R_i)+R_i^2-R_o^2)}{(R_o^4-R_i^4)\ln(R_o/R_i)-(R_i^2-R_o^2)^2}$. The total non-orifice flux coefficient $C := c_{in} + c_{out}$ varies according to the angles of the non-orifice ports, those connecting the actuator are non-orifice ports in the figure, to the spool axis.

where Q is the flow rate, ρ is the fluid density, θ is the vena contracta angle, c_c is the contraction coefficient, μ is the fluid viscosity, L is the damping length, C is the total non-orifice flux coefficient, and α is a geometry constant. A_o is the orifice area whose sign coincides with the spool displacement. For instance, Fig. 1 shows the case where $A_o > 0$. In Eq. (1), the second term $-2\frac{\rho\cos\theta}{c_c A_o}Q^2$ represents the conventionally recognized steady flow forces [1]; The third term $-\alpha L\mu Q$ stands for the viscosity effect that can be manipulated by α and L; the first term $sgn(A_o)CQ^2$ denotes the non-orifice flux effect that can be controlled by C. C, L, α are the design parameters determined by the valve geometry. Note that the second term itself cannot generally be manipulated. Substituting the orifice equation $Q = c_d A_o\sqrt{\frac{2P}{\rho}}$, Eq. (1) can be normalized as,

$$F_{steady} = \kappa C\left(sgn(A)A^2 - (\frac{\kappa_0}{C} + \frac{\kappa_1\alpha L}{C})A\right) \tag{2}$$

where $\kappa = \frac{2c_d^2 P A_{max}^2}{\rho}$, $\kappa_0 = \frac{2\rho\cos\theta}{c_d A_{max}}$, $\kappa_1 = \frac{\mu}{c_d A_{max}}\sqrt{\frac{\rho}{2P}}$, in which A_{max} denotes the allowed maximum orifice area, and the normalized orifice area $A \in [-1, 1]$. $\kappa, \kappa_0, \kappa_1$ are constant provided that P and μ are not perturbed.

Next we need consider what is the appropriate objective function to be optimized for the unstable valve design. Ideally it is preferred that the steady state flow forces is identically zero over the full range of the orifice open. Therefore, The objective function could be so chosen that the steady flow force range is minimized. Because F_{steady} is an odd function of A, the range is linearly associated with $\max(F_{steady})$. In addition, the overall geometric dimension, in particular the damping length L, should be restricted within acceptable values. However note that in Eq. (2), L and α are always multiplied together. Once $(\alpha L)_{opt}$ is obtained, the values of L and R_i, R_o can be assigned so that $L_{opt}\alpha_{opt} = (\alpha L)_{opt}$ can minimize the overall dimension of the valve. Therefore, the objective function can be chosen to be,

$$\min_{C>0,-\alpha L>0} : \max_{A\in[-1,1]} : F_{steady}, \tag{3}$$

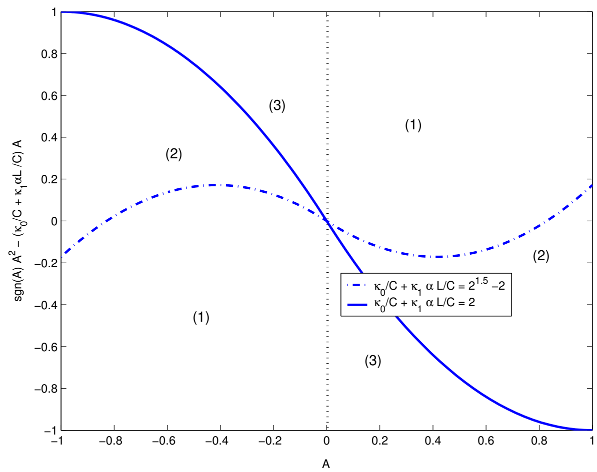

Fig. 2. $\frac{F_{steady}}{\kappa C}$ in a function of $A \in [-1, 1]$.

From Fig. 2 and Eq. (2), $\max_{A\in[-1,1]} F_{steady}(A, \alpha L, C)$ occurs at one of the three situations, 1) $A = 1$, 2) $A = -\frac{1}{2}(\frac{\kappa_0}{C} + \frac{\kappa_1\alpha L}{C})$, or 3) $A = -1$. Case 1) is applicable when $\frac{\kappa_0}{C} + \frac{\kappa_1\alpha L}{C} \le 2\sqrt{2} - 2$, case 2) is applicable when $2\sqrt{2} - 2 < \frac{\kappa_0}{C} + \frac{\kappa_1\alpha L}{C} \le 2$, and case 3) is applicable when $\frac{\kappa_0}{C} + \frac{\kappa_1\alpha L}{C} \le 2\sqrt{2} - 2$. The domains $Dom_1, Dom_2, Dom_3 \subset \{(\alpha L < 0, C > 0)\}$ in which the three cases are applicable are shown in Fig. 2.

$$\max_A F_{steady} = \begin{cases} \kappa(C - \kappa_0 - \kappa_1\alpha L) & \text{case 1: if } (L, C) \in Dom_1, \\ \frac{\kappa(\kappa_0+\kappa_1\alpha L)^2}{2C} & \text{case 2: if } (L, C) \in Dom_2 \\ \kappa(-C + \kappa_0 + \kappa_1\alpha L) & \text{case 3: if } (L, C) \in Dom_3 \end{cases} \tag{4}$$

The optimization problems corresponding to the original min-max problem in (3) in the 3 domains are:

$$\min_{(\alpha L, C)\in Dom_1} : \kappa(C - \kappa_0 - \kappa_1\alpha L) \tag{5}$$

$$\min_{(\alpha L, C)\in Dom_2} : \frac{\kappa(\kappa_0 + \kappa_1\alpha L)^2}{2C} \tag{6}$$

$$\min_{(\alpha L, C)\in Dom_3} : \kappa(-C + \kappa_0 + \kappa_1\alpha L) \tag{7}$$

Notice that each of the subproblems (5)-(7) is convex. It is because all the inequality constraints are linear, and are the objective functions in Eqs. (5)(7). The Hessian matrix of the objective function in (6) is positive semi-definite, so the objective function is convex as well. These subproblems can be easily solved independently according to the Kuhn-Tucker sufficient condition. Because of convexity, the

$$F_{steady}(A_o \geq 0) = 0.25\chi C(1+\delta_A)^2(\bar{P}+W_P\delta_P) - 0.5\chi_0(1+\delta_A)(\bar{P}+W_P\delta_P) - 0.5\chi_1\alpha L(1+\delta_A)(\bar{\mu}+W_\mu\delta_\mu)\sqrt{\bar{P}+W_P\delta_P}$$
$$F_{steady}(A_o \leq 0) = -0.25\chi C(-1+\delta_A)^2(\bar{P}+W_P\delta_P) - 0.5\chi_0(-1+\delta_A)(\bar{P}+W_P\delta_P) - 0.5\chi_1\alpha L(-1+\delta_A)(\bar{\mu}+W_\mu\delta_\mu)\sqrt{\bar{P}+W_P\delta_P} \quad (8)$$

$$\begin{aligned} F_{steady} = & \pm(0.25\chi\bar{P}C - 0.5\chi_0\bar{P} - 0.5\chi_1\sqrt{\bar{P}}\bar{\mu}\alpha L) + (-0.5\chi_0\bar{P} + 0.5\chi\bar{P}C \mp 0.5\chi_1\bar{\mu}\sqrt{\bar{P}}\alpha L)\delta_A \\ & \pm(-0.5\chi_0 W_P + 0.25\chi W_p C - 0.5\chi_1\bar{\mu}W_P D_P\alpha L)\delta_P + (-0.5\chi_0 W_P + 0.5\chi W_P C - 0.5\chi_1\bar{\mu}D_P W_P L\alpha)\delta_{AP} \\ & \mp 0.5\chi 1 W_\mu\alpha L\delta_\mu \pm 0.25\chi\bar{P}C\delta_{AA} \pm 0.5\chi_1 W_P W_\mu D_P\alpha L\delta_{P\mu} \pm 0.25\chi W_P C\delta_{AAP} \\ & - 0.5\chi_1\sqrt{\bar{P}}W_\mu\alpha L\delta_{A\mu} - 0.5\chi_1 D_P W_P W_\mu\alpha L\delta_{AP\mu} \end{aligned} \quad (9)$$

optimal solution for each subproblem is global in its feasible set.

Denote the nominal optimal solutions by $(\alpha L)_{opt}, C_{opt}$. We will next discuss the case in which the operating condition is perturbed.

III. ROBUST OPTIMAL DESIGN

A. LFT representation

In practice some operating conditions in Eq. (2) can be varying within a certain range, like pressure drop across the orifices P and the dynamic viscosity μ. On the assumption of constant pressure supply P_s, the perturbation of P is due to the varying load pressure. It is well known that μ can dramatically change as a function of the temperature of the hydraulic systems. Define $P := \bar{P} + W_P\delta_P$, and $\mu := \bar{\mu} + W_\mu\delta_\mu$ where $\bar{P}, \bar{\mu}$ are the nominal pressure and the nominal dynamic viscosity, $W_p, W_\mu \in \mathcal{R}^+$ are the corresponding weighting functions, and $\delta_P \in B_\delta$ and $\delta_\mu \in B_\delta$ are the corresponding perturbations, in which $B_\delta := \{\delta \in R : |\delta| \leq 1\}$. It is convenient to represent A_o as the perturbations, i.e., $A_o = \{A_{max}(0.5+0.5\delta_A)\} \cup \{A_{max}(-0.5+0.5\delta_A)\}$ where $\delta_A \in B_\delta$. Hence, F_{steady} can be expressed in Eq. (8) where $\chi = \frac{2c_d^2 A_{max}^2}{\rho}$, $\chi_0 = 4c_d\cos\theta A_{max}$, $\chi_1 = \frac{\sqrt{2}A_{max}c_d}{\sqrt{\rho}}$.

In addition, *the mean value theorem* gives that there exist $\{P^* : P^* \in \bar{P} + W_P\delta_P\}$ so that $\sqrt{\bar{P}+W_P\delta_P} = \sqrt{\bar{P}} + W_P D_P(P^*)\delta_P$ where $D_P(P^*)$ is the derivative of $\sqrt{P}$ at P^*. For simplicity, $D_P(P^*)$ is denoted by D_P. Then Eq. (8) can be written as the form in Eq. (9), in which $\delta_{ij} = \delta_i\delta_j$, $\delta_{ijk} = \delta_i\delta_j\delta_k$, in which $\underset{m=i,j,k}{\delta_m} \in \{\delta_A, \delta_P, \delta_\mu\}$. For instance, $\delta_{AP} = \delta_A\delta_P$, and $\delta_{AP\mu} = \delta_A\delta_P\delta_\mu$. Note that $\pm$ and $\mp$ reflect the different representations of F_{steady} for different range of A_o. The upper sign corresponds to $A_o \geq 0$ while the lower sign to $A_o \leq 0$.

The research aims at designing an unstable valve with a better robust performance. In order to facilitate the robust analysis and synthesis, we adopt an approach to represent the original problem by its equivalence, the interconnection of the linear fractional transformation (LFT), as shown in Fig. 3. That is to say, all perturbations are included in Δ, and all the control variables, C, L, and α, are manipulated into a controller K. From Fig. 3, the closed-loop perturbed system is given by

$$e = F_{steady} = \mathcal{F}_l(\mathcal{F}_u(M,\Delta),K)\cdot d \quad (10)$$

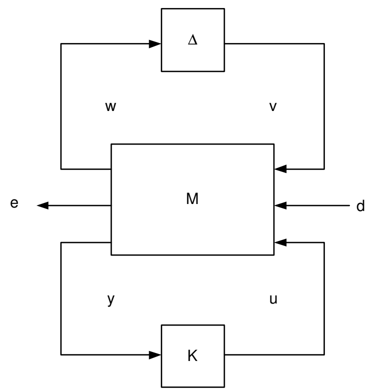

Fig. 3. LFT interconnection of the perturbed closed-loop system

in which we choose $\Delta := diag(\delta_A, \delta_P, \delta_\mu, \delta_{AP}, \delta_{A\mu}, \delta_{P\mu}, \delta_{AA}, \delta_{AAP}, \delta_{AP\mu}) \subset B_\Delta \subset \mathcal{R}^{9\times 9}$ where $B_\Delta := \{\Delta : \bar{\sigma}(\Delta) \leq 1\}$, $K := [C \quad \alpha L] \in \mathcal{R}^{1\times 2}$, $d := 1 \in \mathcal{R}$, M is a real compatible matrix with the form as follows: $M := \begin{bmatrix} M_{11} & M_{12} & M_{13} \\ M_{21} & M_{22} & M_{23} \\ M_{31} & M_{32} & M_{33} \end{bmatrix} \in \mathcal{R}^{(9+1+2)\times(9+1+1)}$.

Then

$$M_{33} = 0_{2\times 1} \qquad M_{32} = 0_{2\times 1} \quad (11)$$
$$M_{12} = 1_{9\times 1} \qquad M_{23} = 1 \quad (12)$$

$$M_{21} = \begin{bmatrix} -0.5\chi_0\bar{P} & \mp 0.5\chi_0 W_P & 0 & -0.5\chi_0 W_P & 0_{1\times 5} \end{bmatrix} \quad (13)$$
$$M_{11} = -M_{13}KM_{31} \quad (14)$$
$$M_{22} = S + M_{23}KT \quad (15)$$
$$M_{31} = \begin{bmatrix} M_{31,A} & M_{31,B} & M_{31,C} \end{bmatrix} \quad (16)$$

where

$$S = [\mp 0.5\chi_0\bar{P}] \quad (17)$$
$$T = \pm[\ 0.25\chi\bar{P} - 0.5\chi_1\sqrt{\bar{P}}\bar{\mu}\ ]^T \quad (18)$$

$$M_{31,A} = \begin{bmatrix} 0.5\chi\bar{P} & \pm 0.25\chi W_P & 0 \\ -0.5\chi_1\sqrt{\bar{P}}\bar{\mu} & \mp 0.5\chi_1\bar{\mu}W_P D_P & \mp 0.5\chi_1\sqrt{\bar{P}}W_\mu \end{bmatrix}$$

$$M_{31,B} = \begin{bmatrix} 0.5\chi W_P & 0 & 0 \\ 0.5\chi_1\bar{\mu}W_P D_P & -0.5\chi_1\sqrt{\bar{P}}W_\mu & \mp 0.5\chi_1 W_P W_\mu D_P \end{bmatrix}$$

$$M_{31,C} = \begin{bmatrix} \pm 0.25\chi \bar{P} & 0 & \pm 0.25\chi W_P \\ 0 & -0.5\chi_1 W_P W_\mu D_P & 0 \end{bmatrix}$$

M_{13} can be arbitrarily chosen. Then Eq. (9) will be exactly represented by Eq. (10).

The robust performance criteria for a given controller K is

$$\gamma(K) := min \left\{ \gamma | \sup_{\Delta \in B_\Delta} \bar{\sigma}(\mathcal{F}_l(\mathcal{F}_u(M, \Delta), K)) \leq \gamma \right\} \tag{19}$$

The optimal value over all controllers is denoted by γ_{opt}. Once we obtain the suboptimal value $\gamma \geq \gamma_{opt}$ and the controller K_{rob}, so that $\gamma(K_{rob}) = \gamma$, the optimal design parameters $C_{rob}, L_{rob}, \alpha_{rob}$ of maximizing the system robustness can be retrieved back from K_{rob}.

B. Synthesizing the optimal controller K_{rob}

As aforementioned, we formulate the optimal design problem of finding the optimal set of geometric parameters into one of designing an optimal robust performance controller for an appropriate static plant with an structured uncertainty. Next, we will discuss how to synthesize the controller. In [6], the authors present a method to synthesize a controller for a static plant. Nevertheless, its robust performance index is of the different form from Eq. (19). In addition, the assumption that the static matrix M must be independent of K is not valid in our problem. Therefore, we cannot directly use the algorithm proposed in [6]. We present a theorem for synthesizing the controller, and the corresponding proof is followed.

Theorem 1: Given $\gamma > 0$, there exists K satisfying

$$\gamma(K) < \gamma \tag{20}$$

where $\gamma(K)$ is defined in Eq. (19), if and only if $\exists z > 0$ satisfying

$$\lambda_{max} \left[V_\perp \left(R(\gamma)^T Z R(\gamma) - \gamma^2 Z \right) V_\perp^T \right] < 0 \tag{21}$$

and

$$\lambda_{max} \left[U_\perp^T \left(R(\gamma) Z^{-1} R(\gamma)^T - \gamma^2 Z^{-1} \right) U_\perp \right] < 0 \tag{22}$$

where $R(\gamma) := \begin{bmatrix} 0 & \gamma M_{12} \\ M_{21} & S \end{bmatrix}, U := \begin{bmatrix} 0 \\ M_{23} \end{bmatrix}, V := \begin{bmatrix} M_{31} & T \end{bmatrix}$, $Z := \{diag(zI_{n_1}, I_{n_2}) | z \in R, z > 0\}$, $U_\perp, V_\perp$ are chosen so that $\begin{bmatrix} U & U_\perp \end{bmatrix}$ and $\begin{bmatrix} V \\ V_\perp \end{bmatrix}$ are both invertible; and $U^T U_\perp = 0$, $V V_\perp^T = 0$.

Proof: First, we choose $\tilde{\Delta} = \Delta/\gamma$, and $\tilde{M}$ based on M as

$$\{\tilde{M} : \tilde{M}_{12} = \gamma M_{12}, \tilde{M}_{ij} = M_{ij} \text{ for } ij \neq 12\} \tag{23}$$

It is easy to show that we can formulate the original robust performance in Eq. (19) into

$$\gamma(K) = \min \left\{ \gamma | \sup_{\bar{\sigma}(\tilde{\Delta}) \leq 1/\gamma} \bar{\sigma}(\mathcal{F}_l(\mathcal{F}_u(\tilde{M}(K, \gamma), \tilde{\Delta}), K)) \leq \gamma \right\} \tag{24}$$

where Δ and $\tilde{\Delta}$ have the different maximum singular value. Again, this problem cannot be solved by the algorithm in [6] because $\tilde{M}(K, \gamma)$ is dependent on K.

Next, we know that this standard robust performance problem can solved by its upper bound [7] though. That is,

$$\gamma(K) \quad = \quad \inf_Z \bar{\sigma}(Z^{1/2} \mathcal{F}_l(\tilde{M}(K, \gamma), K) Z^{-1/2}) \tag{25}$$

where $Z := \{diag(zI_{n_1}, I_{n_2}) | z \in R, z > 0\}$. We have

$$\mathcal{F}_l(\tilde{M}(K, \gamma), K) = \begin{bmatrix} M_{11} & \gamma M_{12} \\ M_{21} & M_{22} \end{bmatrix} + \begin{bmatrix} M_{13} \\ M_{23} \end{bmatrix} K(I - M_{33}K)^{-1} \begin{bmatrix} M_{31} & M_{32} \end{bmatrix} \tag{26}$$

Substituting M_{ij} in Eq. (26) with Eqs. (11)-(15) yields that $\mathcal{F}_l(\tilde{M}, K)$ is a linear function of K,

$$\mathcal{F}_l(\tilde{M}, K) = \underbrace{\begin{bmatrix} 0 & \gamma M_{12} \\ M_{21} & S \end{bmatrix}}_{R(\gamma)} + \underbrace{\begin{bmatrix} 0 \\ M_{23} \end{bmatrix}}_{U} K \underbrace{\begin{bmatrix} M_{31} & T \end{bmatrix}}_{V} \tag{27}$$

Finally, we substitute $\mathcal{F}_l(\tilde{M}, K)$ in Eq. (25) with Eq. (27), and it is easy to show that the theorem holds. ■

Eq. (21) can be equivalently written as $\lambda_{max}(z\Psi_1 + \Psi_2) < 0$ where $\Psi_1 = V_\perp \begin{bmatrix} -\gamma^2 I_{n_1} & 0 \\ 0 & \gamma^2 M_{12}^T M_{12} - I_{n_2} \end{bmatrix} V_\perp^T$ and $\Psi_2 = V_\perp \begin{bmatrix} M_{21}^T M_{21} - I_{n_1} & M_{21}^T S \\ S^T M_{21} & S^T S - \gamma^2 I_{n_2} \end{bmatrix} V_\perp^T$. Similarly, Eq. (22) can be written as $\lambda_{max}(z^{-1}\Phi_1 + \Phi_2) < 0$ where $\Phi_1 = U_\perp^T \begin{bmatrix} -\gamma^2 I_{n1} & 0 \\ 0 & M_{21} M_{21}^T - I_{n_2} \end{bmatrix} U_\perp$ and $\Phi_2 = U_\perp^T \begin{bmatrix} M_{12} M_{12}^T - I_{n1} & M_{12} S^T \\ S M_{12}^T & S S^T - \gamma^2 I_{n_2} \end{bmatrix} U_\perp$. The maximum eigenvalue is a convex function of its argument that is affine in z or z^{-1} in this case. It has been proven in [7] that the z sets satisfying Eqs. (21) and (22) are open intervals in the real line. Therefore, we can choose a γ to check if the intervals intersect, and to minimize the intersected interval.

Once z, γ are obtained, K can be synthesized by the following algorithm that can be derived on the basis of [6]

$$\begin{aligned}
T_1 :=& (U_\perp^T Z^{-1} U_\perp)^{-1/2} U_\perp^T R(\gamma) V_\perp^T (V_\perp Z V_\perp^T)^{-1/2} \\
T_2 :=& (U^T Z U)^{-1/2} U^T R(\gamma) V_\perp^T (V_\perp Z V_\perp^T)^{-1/2} \\
T_3 :=& (U_\perp^T Z^{-1} U_\perp)^{-1/2} U_\perp^T R(\gamma) V^T (V Z^{-1} V^T)^{-1/2} \\
Q_1 :=& -T_2 (\gamma^2 I - T_1^T T_1)^{-1/2} T_1 (\gamma^2 I - T_1 T_1^T)^{1/2} T_3 \\
Q_2 :=& Q_1 - (U^T Z U)^{-1/2} U^T Z R(\gamma) Z^{-1} V^T (V Z^{-1} V^T)^{-1/2} \\
K :=& (U^T Z U)^{-1/2} Q_2 (V Z^{-1} V^T)^{-1/2}
\end{aligned} \tag{28}$$

IV. Case study

In this section, a case study is presented in order to compare the solution sets from the nominal optimal method with ones from the robust method. Suppose the supply pressure

W_P	W_μ	$(\alpha L)_{rob}$	C_{rob}	γ
0	0	-1.1435×10^6	5.82×10^{-9}	0.0156
$0.01\bar{P}$	$0.01\bar{\mu}$	-1.1431×10^6	4.54×10^3	4.3
$0.125\bar{P}$	$0.125\bar{\mu}$	-1.062×10^6	7.29×10^5	51.6
$0.25\bar{P}$	$0.25\bar{\mu}$	-0.707×10^6	2.83×10^6	91.8
$0.375\bar{P}$	$0.375\bar{\mu}$	-0.458×10^6	4.31×10^6	116.7
$0.5\bar{P}$	$0.5\bar{\mu}$	-0.315×10^6	5.18×10^6	134.8

TABLE I

ROBUST OPTIMAL SOLUTION SETS AND THEIR CORRESPONDING ROBUST PERFORMANCES TO VARIOUS PERTURBATION.

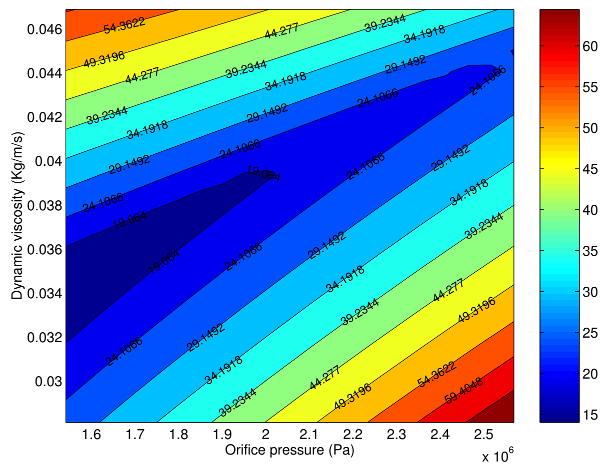

Fig. 4. The contour of $||F_{steady}||_\infty$ with respect to $P \in [0.75\bar{P}, 1.25\bar{P}]$ and $\mu \in [0.75\bar{\mu}, 1.25\bar{\mu}]$ for the corresponding robust solution $(C, \alpha L) = (2.83 \times 10^6, -0.707 \times 10^6)$. The worst case performance is $\sup_{rob} := \sup\limits_{P,\mu}(||F_{steady}||_\infty) \approx 70.0$.

$P_s = 5.15 \times 10^6 Pa(800psi)$ and the load pressure $P_l = 1.38 \times 10^6 Pa(200psi)$, then the nominal pressure differences across both orifices are $\bar{P} = 2.07 \times 10^6 Pa(300psi)$. Mobil DTE Oil 970391 is used in the hydraulic system. The nominal dynamic viscosity $\bar{\mu} = 0.0375 kg/m/s$ at $40°C$ and $\rho = 871 kg/m^3$. The other variables are chosen conventionally as $c_d = 0.6$, $A_{max} = 1.5 \times 10^{-4} m^2$, $\theta = 69°$. On the assumption that P_s is constant, the pressure drop P can be perturbed due to the variation of the load. Suppose we know $W_P \leq 0.5\bar{P}$. In addition, the hydraulic system experiences the temperature fluctuation. Based on [1], we have the approximate equation of the viscosity w.r.t. the temperature,

$$\mu = \mu_0 e^{-\lambda(T - T_0)} \tag{29}$$

where T_0 is the reference temperature, and μ_0 is the dynamic viscosity at T_0, e.g. we can set $T_0 = 40°C$ and $\mu_0 = \bar{\mu}$. The constant $\lambda = 0.0311(°C)^{-1}$ can be specified from the data sheet of Mobil DTE Oil. Suppose that the temperature varies within $27°C \sim 60°C$, then we can ensure $W_\mu \leq 0.5\bar{\mu}$. The comparison of the solutions by optimal design and robust design is presented as follows,

1) Apply optimal design approach in section II. We have $C_{opt} = 1.1 \times 10^{-12}$, $(\alpha L)_{opt} = -1.1435 \times 10^6$. The minimum of the objective function is 5.16×10^{-7}.
2) Robust design is implemented as well, according to the algorithm in section III. For various W_P and W_μ where $W_P \leq 0.5\bar{P}$ and $W_\mu \leq 0.5\bar{\mu}$, the optimal sets $(\alpha L)_{rob}$ and C_{rob} are obtained, as can be seen in Table I. The corresponding robust performances $\gamma(K_{rob}) \leq \gamma$ are also calculated.

There are several observations that can be obtained in Table I. (1) Under the condition of zero perturbation ($W_P = 0$ and $W_\mu = 0$), the robust optimal solution sets are almost exactly same as the ones from the nominal optimal method. This directly verifies the validity of the robust design algorithm. Once the perturbation is applied, however, the robust optimal sets start to divert from the nominal optimal values. As shown in Table I, only 1% of the operating condition variation change the optimal solution dramatically, as well as the performance. (2) The extent to which the robust optimal solutions diverge from the nominal solutions is determined by the degree of the uncertainty. In Table I, as the weighting functions of uncertainties (W_P, W_μ) increase from (0,0) to $(0.5\bar{P}, 0.5\bar{\mu})$, the optimal set $(\alpha L, C_{rob})$ diverts from the nominal optimum $(-1.1435 \times 10^6, 0)$ to $(-2.75 \times 10^5, 4.43 \times 10^6)$ monotonically. Physically speaking, under the nominal operating condition, the unstable valve tends to exclusively utilize the viscosity effect to zero the steady flow forces in the full range of the orifice open. However, once confronted with the perturbations, the optimal solutions of compensating the steady flow forces should take into account both the viscosity effect and the non-orifice flux effect simultaneously. (3) We can compare the robust performance for various perturbations. For zero perturbations, note that the steady forces are nearly zero for the full range of orifice opening. However, regardless of robust optimal design effort, γ always increases for enlarged perturbations. That is to say, there is always a larger steady flow force range for the larger uncertainty event though this range has already been minimized. This should not be a surprising result.

In order to visualize the benefit of the robust design method, Monte Carlo simulations are conducted. We consider a scenario where the uncertainty weights are $W_P = 0.25\bar{P}$ and $W_\mu = 0.25\bar{\mu}$. Then the pressure drop across the orifice P and the dynamic viscosity μ are randomly selected within the range, as can be seen in Figs. 4-6. Given P and μ, $||F_{steady}||_\infty$ can be computed from Eq. (4). The contour of $||F_{steady}||_\infty$ in the (P, μ) domain are plotted for various design parameters. Specifically, the robust optimal solutions $(C_{rob}, (\alpha L)_{rob})$ are used in Fig. 4, while the nominal optimal solutions $(C_{opt}, (\alpha L)_{opt})$ are used in Fig. 5. We also consider another group of parameters by which the valve is designed to be stable, namely $\alpha L > 0$, as shown in Fig. 6. The worst case performances $\sup\limits_{P,\mu}(||F_{steady}||_\infty)$ are considered. The fact that $\sup_{rob} < \sup_{opt} < \sup_{stbl}$ where $\sup_{rob}, \sup_{opt}, \sup_{stbl}$ are defined as the worst case

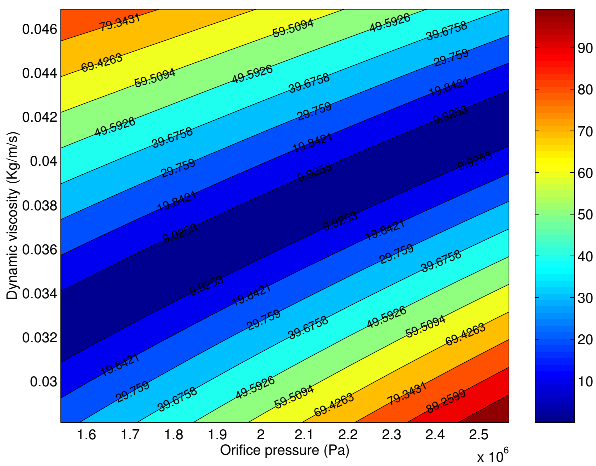

Fig. 5. The contour of $||F_{steady}||_\infty$ with respect to $P \in [0.75\bar{P}, 1.25\bar{P}]$ and $\mu \in [0.75\bar{\mu}, 1.25\bar{\mu}]$ for the nominal optimal solution $(C, \alpha L) = (0, -1.1435 \times 10^6)$. The worst case performance is $\sup_{opt} := \sup_{P,\mu}{}_{opt}(||F_{steady}||_\infty) \approx 109.4$.

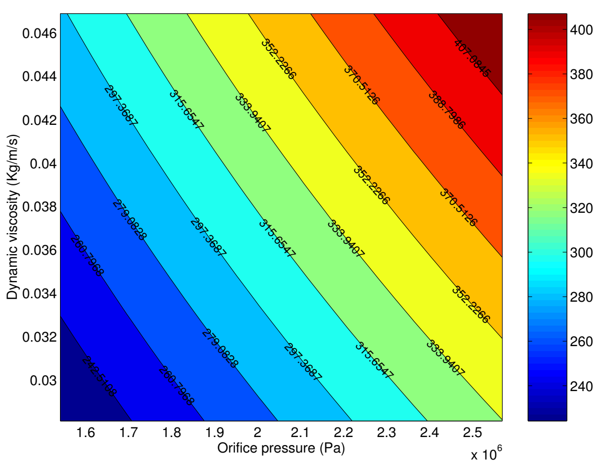

Fig. 6. The contour of $||F_{steady}||_\infty$ with respect to $P \in [0.75\bar{P}, 1.25\bar{P}]$ and $\mu \in [0.75\bar{\mu}, 1.25\bar{\mu}]$ for $(C, \alpha L) = (2.83 \times 10^6, 0.707 \times 10^6)$, which corresponds to a stable valve. The worst case performance is $\sup_{stbl} := \sup_{P,\mu}(||F_{steady}||_\infty) \approx 425.2$.

performance for the cases in Fig. 4,5, and 6 respectively, confirms that (1) nominal optimal solution does not provide the best performance under the perturbations, thus necessitating the robust design algorithm; (2) the stable valve has much worse performance, greater than 3 times in this case, than the unstable valve. Therefore, the unstable valve tends to be more robust than the stable valve.

In addition, the worst case scenario calculated from the robust algorithm in Section III-B, is $(P, \mu) = (1.25\bar{P}, 0.75\bar{\mu})$, which coincides very well with the Monte Carlo simulation results using the robust solution, as shown in Fig. 4. Nevertheless, note that the worst case performance value of the Monte Carlo simulation $\sup_{rob} \approx 70.0$ is about 80% of the robust performance value provided by the robust optimal design method, namely $\gamma = 91.8$ in Table I. This can be explained by the fact that the diagonal elements in the constructed perturbation matrix Δ, which is defined in Section III-A, are partially correlated, but the worst case perturbation of the robust optimal method would not take it into account, thus being infeasible. The conservative γ yields a reasonable upper bound though.

V. Conclusion

Unstable valve is designed for improving the response performance of single stage electrohydraulic valves in the high frequency applications. In this paper, based on our previous research effort of precisely modeling the flow forces in a valve, we present the optimal methods concerning unstable valve design. The nominal optimal method is proposed to facilitate design under the nominal operating conditions. Furthermore, we pay more attention to realize the robust optimal design with taking into account perturbation. We formulate the robust optimal design problem of finding the optimal set of geometric parameters into designing an optimal controller to optimize the robust performance of a static plant with structured uncertainty. The case study shows that (1) unlike under the nominal condition where the steady forces can be totally neutralized by using the viscosity effect, we should depend on both viscosity effect and non-orifice flux effect to optimize the steady flow force range if the uncertainty in the system is expected; (2) the robust design method is effective to synthesize a group of design parameters, which can provide the optimal performance that is generally not provided by the nominal optimal solutions.

The robust optimal design method has currently been utilized to design the prototype of an unstable valve. The further effort will be made to investigate the lumped system of the unstable valve and solenoid actuators, and to design the controller to optimize the overall performance.

References

[1] H. E. Merritt, *Hydraulic Control System*. John Wiley and Sons, 1967.
[2] K. Krishnaswamy and P. Y. Li, "On using unstable electrolydraulic valves for control," *ASME Journal of Dynamic Systems,Measurement and Control*, vol. 124, no. 1, pp. 182–190, March 2002.
[3] Q. Yuan and P. Y. Li, "An experimental study on the use of unstable electrolydraulic valves for control," in *Proceedings of the 2002 American Control Conference*, Anchorage, Alaska, May 2002, pp. 4843–8.
[4] ——, "Using viscosity to improve spool agility," in *Proceedings of the 2002 Power Transmission and Motion Control (PTMC), Bath, UK*, Sep. 11-13 2002, editors: C.R. Burrows, K.A. Edge, pp 263-286, Professional Engineering Publishing LTD., London, UK, 2002.
[5] ——, "Modeling and experimental study of flow forces for unstable valve design," in *Proceedings of the 2003 ASME international mechanical engineering congress*, Washington DC., USA, Nov. 15 -21 2003.
[6] R.Smith and A. Packard, "Optimal control of perturbed linear static systems," *IEEE transactions of automatic control*, vol. 41, no. 4, pp. 579–584, April 1996.
[7] A. Packard and J. C. Doyle, "The complex structured singular value," *Automatica*, vol. 29, no. 1, 1993.